UC Riverside
UC Riverside Electronic Theses and Dissertations

Title

The Synthesis, Characterization, and Antimicrobial Analysis of Copper Nanoparticle Doped Graphene-Matrix Material

Permalink

Author

Sandu, Cristina-Mihaela

Publication Date

2021

Peer reviewed|Thesis/dissertation

UNIVERSITY OF CALIFORNIA
RIVERSIDE

The Synthesis, Characterization, and Antimicrobial Analysis of Copper Nanoparticle
Doped Graphene-Matrix Material

A Thesis submitted in partial satisfaction
of the requirements for the degree of

Master of Science

in

Materials Science and Engineering

by

Cristina-Mihaela Sandu

March 2021

Thesis Committee:
        Dr. Cengiz Ozkan, Co-Chairperson
        Dr. Mihri Ozkan, Co-Chairperson
        Dr. Marko Princevac
        Dr. Kambiz Vafai

The Thesis of Cristina-Mihaela Sandu is approved:

_____

Committee Co-Chairperson

Committee Co-Chairperson

University of California, Riverside

Acknowledgements

I would like to thank Dr. Cengiz Ozkan and Dr. Mihri Ozkan for their support and for the opportunity to broaden and grow my intellectual ability in their lab. The value of this experience to me is incalculable. Thank you to the rest of my committee, Dr. Marko Princevac and Dr. Kambiz Vafai for their understanding and support. I would like to thank all the students in the Ozkan lab, especially Andy Patalano and Fabian Villalobos for their help and guidance. A special thank you to my parents, Nick and Mary Sandu for all their sacrifices, as well as my good friend Robert Ionescu for encouraging and supporting me.

Table of Contents

Chapter 1. Introduction

Chapter 2. Scalable Copper Graphene-Matrix Sponge

Chapter 3. Antimicrobial Susceptibility: Disk-Diffusion Method

Chapter 4. Viability and Cell Proliferation Assays

Chapter 5. Liquid Broth Culture

Chapter 6. Modified Cytotoxicity Fluorescence Assay

List of Figures

Chapter 1.

Introduction

Pathogenic microbes pose a serious threat to public health. Specifically, antibiotic abuse is creating new strains of antibiotic resistant bacteria and creating a public health crisis. There are many health risks associated with the overuse of antibiotics. Their broad bactericidal effects can disrupt an individual's symbiotic relationship with beneficial bacteria [1]. Furthermore, antibiotics can be toxic to human and create serious side effects from skin sensitivity to organ failure [2]. In addition to some microbes' inherent antibiotic resistive genes, microbes evolve and mutate quickly thereby quickly producing antibiotic resistance. Antibiotic sensitive bacteria are able to acquire antibiotic resistance genes via horizontal gene transfer, causing the organism to then become resistant to specific classes of antibiotics, further complicating treatment [3]. It is therefore of great interest in the scientific community to examine other methods of infectious disease prevention and treatment.

The common solution to prevent pathogenic infections tends to rely on organic disinfectants or drugs, however this solution may lead to drug resistance and can harm the environment. Since about 80% of microbes are transmitted through surface contact, another approach to preventing the spread of harmful microbes is to develop surface technology which not only is bactericidal, but also overcomes the concern of drug resistance and is safe for the environment [4]. Additionally, most efforts dedicated to antimicrobial surface technologies are limited by the exposure hazard of the diffusion of

1

toxic agents or, as the case of cationic polymers, steric hindrance or interaction interference with the bacteria due to the immobilization of the agent [5] . Therefore, an effective surface-immobilized antimicrobial coating material which eliminates patient exposure to the active agents is necessary.

Since the introduction of the GAIN Act in 2012, there has been new stimulated interest in the battle against bacteria, however no significant strides have been made yet [3]. Growing resistance to antibiotics continues to be a devastating public health problem. Attempts to tackle the problem involve research teams at the Massachusetts Institute of Technology (MIT) who utilize a type of phage therapy to target antibiotic resistance genes directly via the CRISPR (clustered, regularly interspaced short palindromic repeats) Cas9 gene editing technology [3]. The engineered phage (a phage is a virus which infects bacteria) delivers the CRISPR Cas9 RNA tool into resistant bacteria, resulting in genomic expression of the CRISPR Cas9 tool which then programs the bacteria to either become sensitive to drugs or to undergo lysis [6]. The CRISPR Cas9 tool encodes a DNA nuclease (DNA degrading enzyme) that recognizes and cleaves specific genes which code for antibiotic resistance [3]. The phage tool selectively kills bacteria with chromosomally integrated resistance genes, while bacteria with plasmid-integrated resistance genes become sensitive and continue to survive, adding a selective pressure which favors sensitive bacteria to resistant bacteria [6]. The surviving bacteria can then be effectively treated with antibiotics. Ironically, the CRISPR Cas9 system is a part of bacteria's natural immune defense against phage attacks [3]. While this tool seems very promising in research, gene therapy is very difficult to implement and apply outside

research labs. Furthermore, it does not prevent the development of antibiotic resistance; there will always be too great a pressure for bacteria to evolve further resistance and survive.

Naturally occurring structures can serve as templates for such bactericidal applications. It has been reported that the nanoscale structure of dragonfly wings may serve as a bactericidal surface [7]. Their natural structure can rupture adjacent microbial cells thereby killing and preventing bacterial growth. These organic templates can be reproduced synthetically and applied to the development of microbicide technologies. It has been observed that the interaction between synthetic nanoparticles and biological cells can be enough to cause cell lysis and death without any other external forces, chemical nor mechanical [8]. This idea is a promising opportunity for the development of novel bactericidal surface technologies which are effective and safe.

Nanomaterials have the capacity to enhance the field of science that relies on public health and sterility, from water treatments, medical devices, and food processing [9]. Metal oxide nanoparticles such as zinc oxide and copper oxide exhibit antimicrobial behavior at different degrees in a variety of materials, forms, and morphologies [7]. The functional activity of nanoparticles is affected by material size, shape, and morphology. Analyzing and characterizing the effects of nanoparticles of varying properties is of current interest in research for biomedical and industrial applications. Medical devices may harbor harmful bacteria which can be deadly for an immune compromised or elderly patient [2]. Bacteria can produce highly resistant biofilms which allow them to survive on such surfaces for long lengths of time. *Staphylococcus aureus* (*S. aureus*) and

Escherichia coli (*E. coli*) are commonly acquired hospital infections that may cause deadly bloodstream, urinary tract, lung, heart, and skin infections [10]. These microbes can be very resistant to conventional antibiotics, requiring the need for novel methods of reducing microbial infections. Metallic nanoparticles have been reported to show antimicrobial activity especially towards pathogenic bacteria such as *E. coli* and *S. aureus* [8] [11]. Antimicrobial effects of the nanoparticle depend on the particle size, stability, and concentration; with the right preparation and application, these particles can hold a promising future in safely reducing infection. Furthermore, graphene based nanomaterials show promising development in the antimicrobial community [7]. Graphene materials have been shown to interact with biomolecules such as proteins, nucleic acids and membranes; these material-microbial interfaces are worthy of analysis in order to further understand the beneficial application of such materials [7].

Here, an economical, scalable and facile sol-gel method to synthesize a metallic copper nanoparticle embedded carbon matrix material (CMAT) is described. Furthermore, CMAT's antimicrobial potential is investigated. CMAT possesses hydrophobic properties as well as high flame resistivity and a high absorption ability of oils. These properties generate a spectrum of prospective CMAT applications ranging from environmental decontamination, biomedical antimicrobial coatings, storage solutions, and air filters.

Chapter 2. Scalable Copper CMAT

2.1 Introduction

Developing safe materials with effective antimicrobial activity, such as nanoparticle surface coatings, is fundamental for public health progress. Carbon based materials have widespread applications ranging from catalysis to remediation [12]. Specifically, activated carbon, characterized by high surface area due to presence of micropores, loaded with metal oxide nanoparticles possess attractive versatile properties [13]. Graphene is a recent carbon based nanomaterial that deserves further investigation and research for such applications. Graphene is a single atom thick sp^2 carbon hexagonal sheet; it can be considered a two-dimensional sheet of graphite [14]. 2-D materials are a topic of interest for researchers because of their scaling down ability. As the scaling-down of electrical components such as field-effect transistors (FETs) reaches design and mechanical thresholds, novel 2-D materials are thus needed to bridge the gap between size and efficiency. Graphene along with other 2-D materials exhibit promising properties for novel applications. Besides their use in convenient technology, energy conservation and restoration are also vital research topics as we continue to observe the detrimental effects of pollution and overconsumption of our natural resources. Green synthesis, or utilizing non-toxic and eco-friendly methods of material synthesis, is an important approach in conservation and nanotechnology which deserves further investigation.

Nanotechnology has vast potential in public health. The combination of nanotechnology and biology can be a powerful force in fighting not only infectious disease and pathogens, but cancer and other genetic disorders as well. Nanoparticles have unique properties relative to their respective bulk material: they exhibit increased

membrane solubility, unique biochemical reactivity, and antimicrobial properties [15]. Metallic nanoparticles therefore have large potential in the engineering and biomedical sciences. Such particles typically range in size between 10 and 500 nanometers; this size can facilitate varying interactions with contact cell surface molecules [15]. It has been reported that silver, copper, and gold nanoparticles exhibit a wide spectrum of antimicrobial activity [15]. The availability and the cost of copper make it a more favorable particle to work with; it shares similar properties to gold and silver as well as antimicrobial properties against a wide range of bacteria and fungi. Copper nanoparticles and their potential in sensors, catalysis, batteries, and superconductors have also been studied [16]. Furthermore, copper nanoparticles exhibit stable shelf lives, antifungal and antibacterial properties. R. Sivaraj et al reported using *Acalypha indica* leaves for the environmentally friendly biosynthesis of copper oxide nanoparticles [17]. It was observed that these naturally synthesized particles not only exhibit antimicrobial properties, but also can aid in treating asthma, pneumonia, and rheumatoid arthritis [17] [18].

Nanopatterns of surfaces such as polymers, titanium oxide, and black silicon and their subsequent bactericidal-contact interactions have been studied for their antimicrobial applications [7]. These surfaces are generally prepared via a top-down method however their high synthesis cost pose a large obstacle in research and development. It is then critical to develop a facile, scalable, environmentally safe, and cost effective method of creating a bactericidal coating for application on common surfaces. Guanshun et al have demonstrated a method for growing ZnO nanopillars by spin coating a layer of ZnO seeds on a substrate, then growing ZnO nanopillars in

aqueous zinc salts [7]. The morphology of these nanostructures is consistent with naturally occurring bactericidal nanostructures on dragonfly wings. The ZnO pillars were observed to have surface bactericidal effects through contact-dependent cell lysis. Furthermore, remote bactericidal effects were also observed. These remote effects can be accounted for by the effects of radicals or reactive oxidative species (ROS) released by ZnO [7]. ZnO nanostructures are able to generate superoxide species by using electrons in their conduction band [7]. Reactive oxide species formed from such semiconductors are quickly lethal to bacteria. However, surface defects in such materials can limit radical generation. Furthermore, electrons or holes may require photo irradiation to form those toxic radicals, which is not always practical in application [7].

Here, the synthesis of a graphene matrix material (formly known as G-sponge) interspersed with metallic nanoparticles via a sol-gel process followed by curing and annealing at high temperatures is described. The process which has been adapted and optimized from Hamed's previous work, allows for an inexpensive, scalable, three-dimensional graphene product which can be doped with various nanoparticles and has potential for many bioengineering and environmental applications [19]. Three-dimensional graphene architectures have great oil absorption as well as hydrophobic properties making such products an excellent candidate not only in environmental decontamination and sustainability applications, but in biological, sensing, and imaging applications as well [20]. Raman spectroscopy, X-Ray Diffraction (XRD), and scanning electron microscopy (SEM) are used for characterization and analysis of the material.

The antimicrobial properties of CMAT are analyzed by a microbiology disk-diffusion method, fluorescent viability and cytotoxicity assays.

2.2 Method

The copper CMAT is synthesized following a sol-gel process followed by curing and annealing. An aqueous solution of deionized water, polyvinyl alcohol, sucrose, and copper nitrate is mixed and stirred at 90C overnight until a gel is formed. The gel is placed in a clean glass beaker and cured in a vacuum oven at 120C for two hours to form the sponge matrix. The matrix is then cut and annealed in a horizontal tube furnace between 500 -1000C with a rate of 10C per minute. under argon and hydrogen gas. The final annealed sponge has a graphitic grey color and is very brittle to the touch.

Figure 2.1: "Sol" step of CMAT synthesis stirred on a hot plate. Final annealed product mechanically pressed into a fine powder (less than 2 micron particles).

2.3 Characterization

CMAT was characterized using Raman Spectroscopy, SEM, and XRD. Figure 2.2 shows the amorphous and highly textured surface of sponge material using SEM imaging. The highly porous architectures of the sponge give the material its low density, high surface area, and light weight properties.
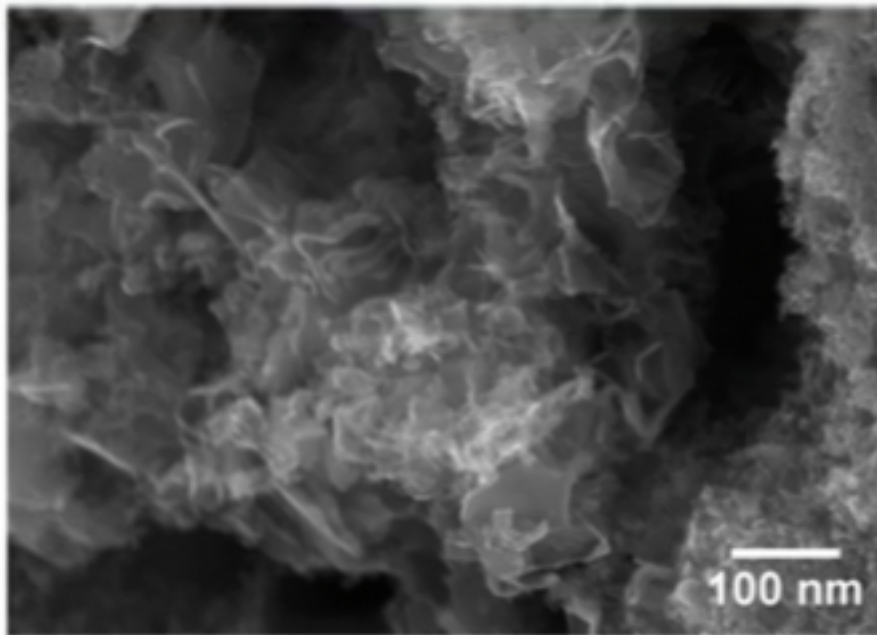
Figure 2.2: High magnification SEM of CMAT surface showing rough, highly porous architectures of CMAT.

Raman-spectrum of CMAT was recorded using a 532nm diode laser and CCD camera. Raman spectroscopy is a nondestructive, standard method for characterization of carbon containing materials. The G peak dispersion of the Raman spectra can be obtained

and correlated with chemical composition, density, and sp^3 content [21]. The multitude

of properties arising from carbon greatly depends on the ratio of sp^2 to sp^3 bonds in the

material. The forms of sp^2 carbon can range from micro-crystalline graphite to glassy

carbon; amorphous carbon can have a mixture of sp^2, sp^3, and sp^1. Sp^2 carbon films

are very intriguing at the nanoscale; specifically, in sensor and electrochemical

applications as well as fuel cells and supercapacitors [21].

Graphite's phonon dispersion has been extensively studied. In defected graphite,

it is crucial to correctly interpret the phonon dispersion around K in order to correctly

analyze the Raman D peak [21]. It has been shown that the dispersion of the D peak

depends on the shape of the phonon branches around K. Piscanec *et al.* showed that the

metallic like characteristic of the electronic structure of graphite is critical when

understanding the D peak [14]. The Kohn anomaly is used to describe the behavior of the

phono dispersion in graphite and essentially describing its electronic band dispersion as

by an isolated graphene sheet where the gap between empty and occupied electronic

states is zero at K and K' in the Brillioun Zone [14].

The Raman spectra is affected by a number of characteristics: bond length and

bond angle disorder, sp^2 chains or rings, and the ratio of sp^2 to sp^3. Also, the spectra is

directly affected by the configuration of the sp^2 phase and indirectly by the quantity of

the sp^2 phase [14] [21]. The configuration of the sp^2 phase can vary independently from

the sp^2 to sp^3 ratio, known as non-uniquness, and this phenomenon may be a result of

annealing after deposition, high temperature deposition or unfiltered deposition methods

[21]. All carbons show shared features in the 800-2000 cm^{-1} area, the G (1560 cm^{-1})

and D (1360 cm^{-1}) peaks which can be seen on the far left of the Raman spectra in

Figure 2.3. The G and D peaks are a result of sp^2 sites; the G peak is in consequence to

ring and chain sp^2 bond stretching whereas the D peak is related to disorder and a result

of cyclic sp^2 atoms [21]. The D peak in the Raman spectra as seen in Figure 2.3 thus

means the presence of sp^2 carbon hexagonal rings and defects [21]. Stage 1 of the

amorphization trajectory of graphite is characterized by the G peak moving from 1581 to

1600 cm^{-1} and an increase in D peak intensity. It can be observed the that G peak in the

Raman Spectra in Figure 2.3 is at about 1560 cm^{-1} therefore the material is not in this

stage of order. Stage 2 is characterized by weaker bonds bringing the G peak to about

1510 cm^{-1} while stage 3 configuration brings the G peak closer to 1570 cm^{-1} due to π

electron confinement in short chains [21]. CMAT is therefore most likely in the stage 3

amorphous carbon configuration.

It is likely that the $2950 cm^{-1}$ mode may be a defect mode induced from local

defect modes [22]. It has been shown by Sato et al. that Raman spectra of carbons from

copper containing starting materials show similar narrow D and G bands and relative

intensities as well as a $2950 cm^{-1}$ band, as observed in the CMAT spectra [22]. The

$2450 cm^{-1}$ peak is concerned with double resonance Raman scattering in phonon

dispersion of two-dimensional graphite [22].

Cu-G
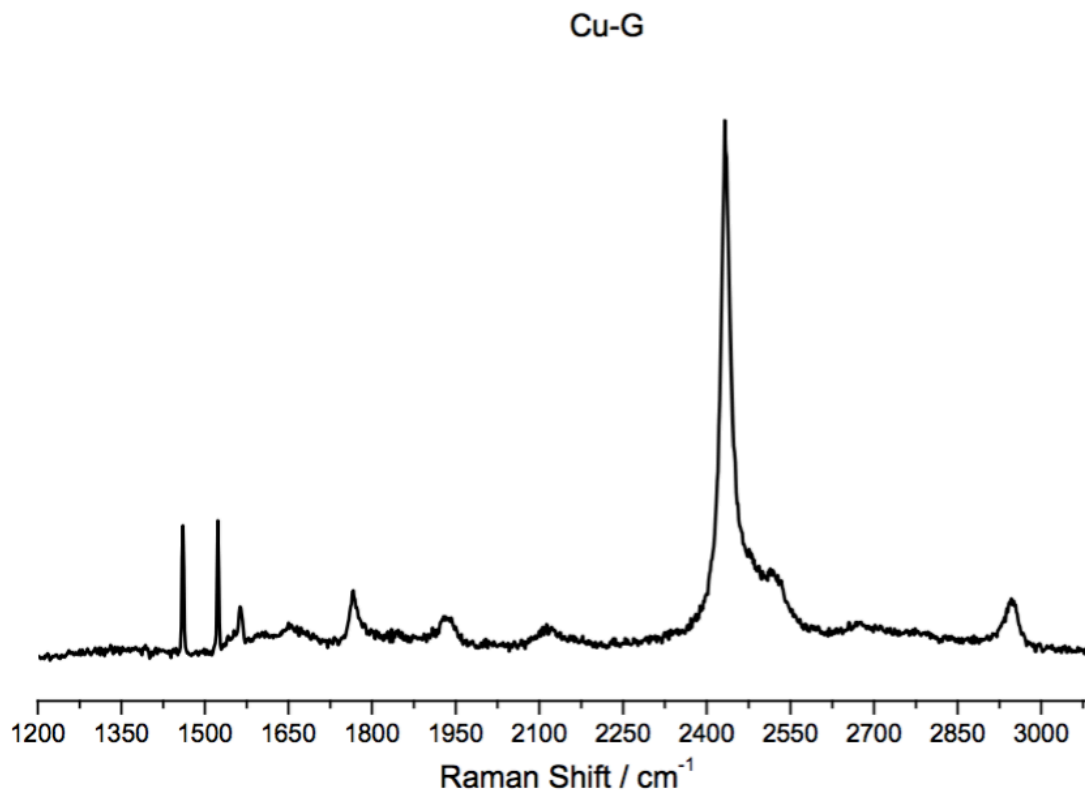
Figure 2.3: Raman spectra of CMAT in arbitrary units.

Crystal structure identification was performed by X-ray diffraction (XRD) analysis. XRD is a convenient tool to analyze the size and shape of the unit cell for a material. Phase identification as well as quantitative analysis is possible with XRD. The diffraction pattern of a compound gives insight on translational symmetry and information on electron density inside the unit cell as well as defects [16]. In Figure 2.4, X-ray diffraction peak at 43 may indicate C (100) signifying reduced graphite oxide. The peaks at 43, 50, and 74 may correspond to (111), (200), and (220) planes of copper [23]. These represent crystal face-centered cubic of copper. The XRD peak at 90 and 95 may

indicate (311) and (222) planes of copper [24]. The sharper peaks in the XRD plot shown in Figure 2.5 suggests higher crystallinity of the final product when sucrose is as a precursor as opposed to glucose.
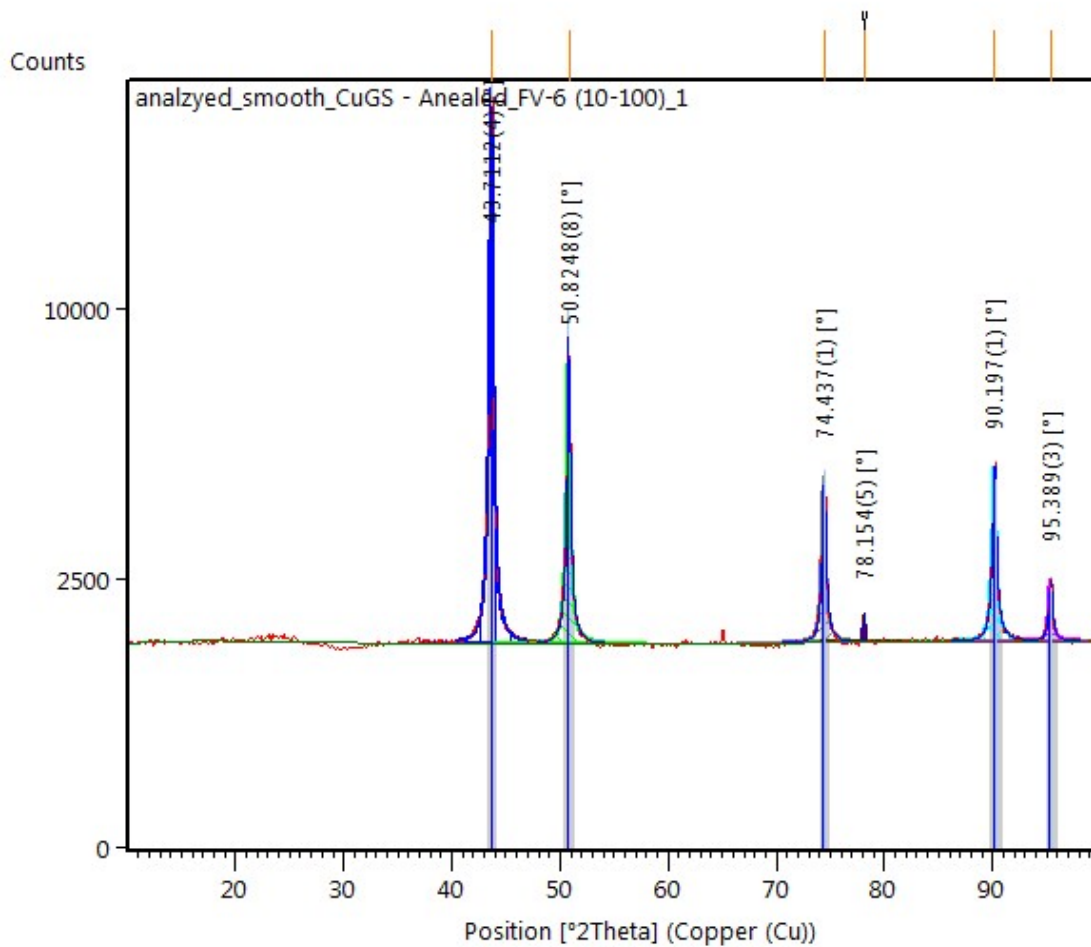
Figure 2.4: XRD peaks of CMAT with sucrose precursor.
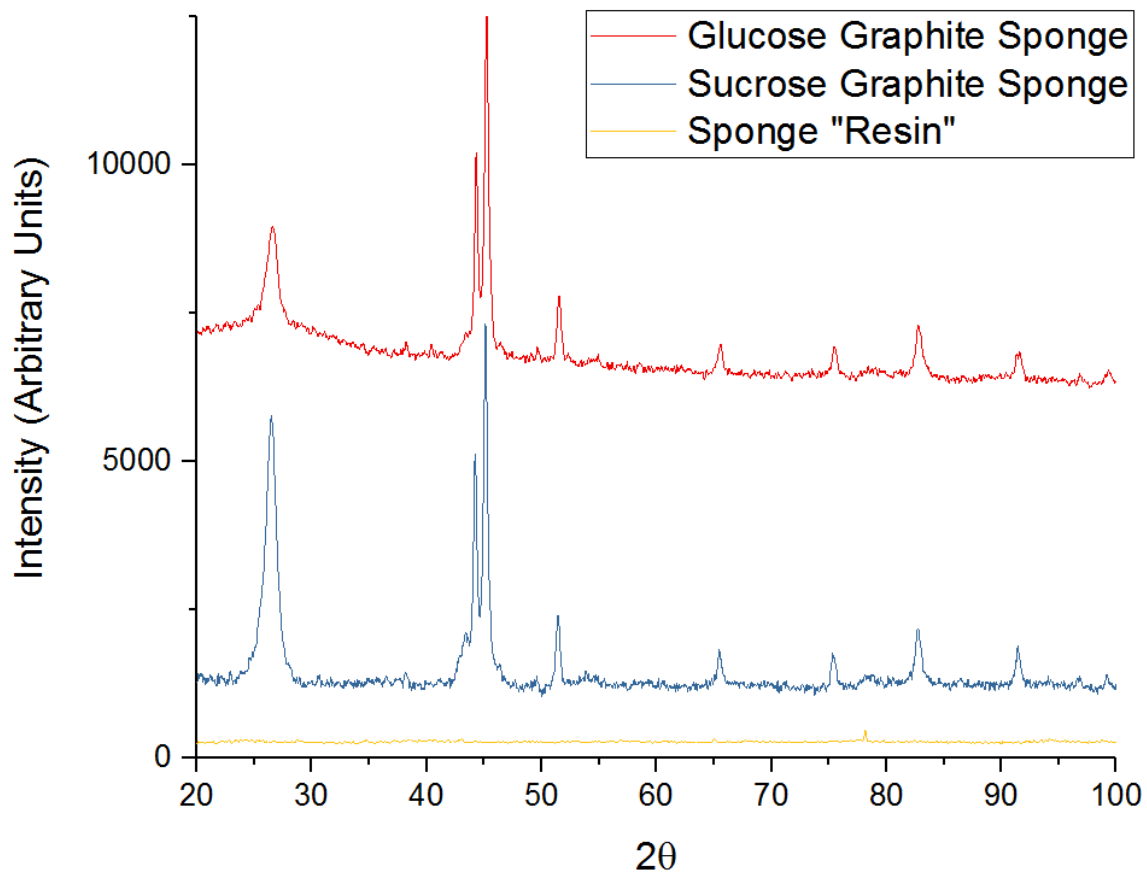
Figure 2.5: Synthesis of CMAT using sucrose as a precursor may yield higher crystallinity, as suggested by the sharper peaks in its XRD plot.

2.4 Conclusion

The synthesis of a scalable carbon matrix embedded with copper nanoparticles and with high porosity is demonstrated following a sol gel process. The synthesis process is facile, inexpensive and easily scalable for a wide spectrum of applications. Characterization of CMAT validating its composition is accomplished using Raman spectroscopy, XRD, and SEM imaging. The material's oil absorption properties and

14

possible antimicrobial properties, which will be investigated next, make it a versatile material for environmental cleaning and decontamination applications.

Chapter 3: Antimicrobial Susceptibility: Disk Diffusion

3.1 Introduction

The gold standard of measuring antimicrobial susceptibility is the Kirby-Bauer Disk Diffusion method of susceptibility. This method allows microbial susceptibility categorization of bacterial isolates against a variety of antimicrobial agents. On a nutrient rich agar petri-dish, a bacterial lawn consisting of the isolated organism is cultured in the presence of antimicrobial agent in question. Minimum inhibitory concentration (MIC) values are determined based on the diameter free of microbial growth (zone of inhibition) around each disk. This data allows for further analysis and characterization of specific antimicrobial agents [3].

Antimicrobial agents can be characterized in terms of its respective bacteriostatic or bactericidal effect, its spectrum of action, and its concentration dependent and time dependent effects on organisms [3]. A bactericidal agent kills organisms rapidly after exposure whereas a bacteriostatic agent only inhibits bacterial growth therefore the number of viable bacteria remains relatively constant. Bactericidal agents are usually the preferred path of action because they produce a quicker response and are less likely to promote microbial resistance. Some bactericidal antimicrobial agents include the physical or mechanical rupture of cell wall and therefore cell death, inhibition of the synthesis of the cell wall or activation of lytic enzymes leading to apoptosis (such as penicillin's

mechanism of action), or other lethal changes in gene expression or inhibition of gene expression [3]. Bacteriostatic drugs may inhibit a metabolic pathway required for growth, but not necessarily required for survival.

Resistance in microbes may be innate, or may be acquired. Acquired resistance can result from transfer of plasmids enclosing resistance genes or from mutation and selection. Random DNA mutations occur regularly; in microbes, the rate of mutation is relatively constant at about 1 in 10^{12} organisms [3]. A random mutation may form resistance to a particular antimicrobial agent: if organisms are exposed to an antimicrobial agent during a mutation period which renders them resistant, the resistant organisms survive and become the prominent strain while the sensitive organisms die off (Figure 3.1). If the organisms are exposed to a suboptimal concentration of the antimicrobial agent, the chances of a mutation and selection of the resistant mutation increases [3]. Therefore, dosage and duration is critical.

Resistance factors, or genes which encode proteins responsible for resistance, can be transferred between organisms in a number of ways including the transfer of plasmids between organisms, or transduction mediated by bacteriophages leading to transfer of DNA between bacterial species. Studies have been done in effort to create drugs which block the expression of resistance factors by developing antisense nucleotides which

16

block transcription of resistance genes [3].
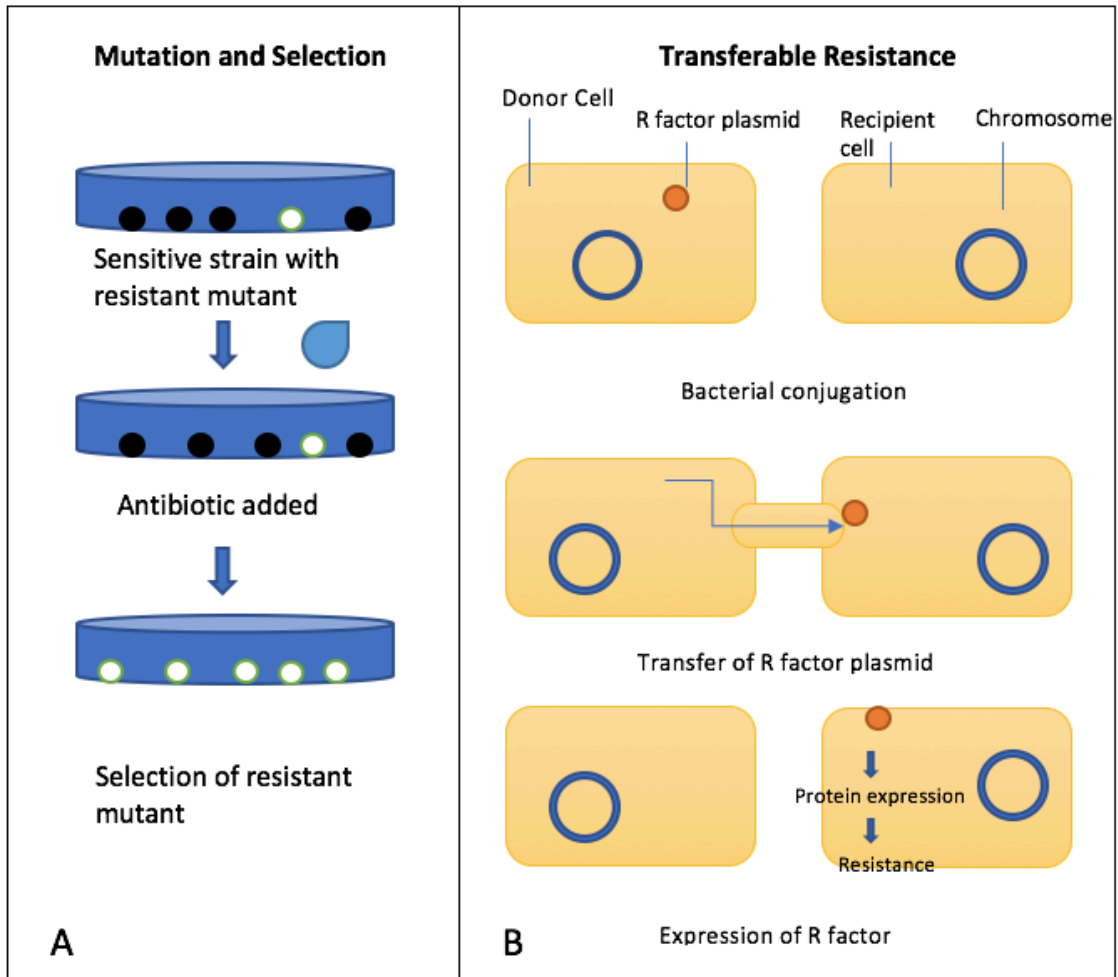
Figure 3.1: Schematic of antibiotic resistance methods. Antibiotic resistance may arise from A) exposure to a resistant mutant or B) bacterial conjugation and exchange of resistance factors in plasmids.

Innate resistance describes an organism's ability to survive a stressor by utilizing its existing genetic script. Regulated genetic factors naturally protect bacteria from antibiotics by induction and transcription of certain efflux genes, biofilm development,

and decreased membrane permeability [25]. Biofilm resistance is a multifactorial innate

mechanism which greatly increases cells' resistance to antibiotics and other bactericidal

factors. During biofilm development, a thick polysaccharide matrix encompasses the

cells and upregulation of antimicrobial factors is observed. The nature of the genotypic

changes of bacteria during biofilm development is not well understood. However, it is

likely that a combination of factors which decrease membrane permeability and the

alteration of target antimicrobial proteins and enzymes play a role in this innate resistance

pathway [10]. Understanding the nature of these pathways is important in developing

novel antimicrobial mechanisms.

3.2 Methods

In order to measure the level of antimicrobial sensitivity of the copper sponge

material, disk-diffusion method was performed. Meuller-Hinton growth media plates

(Hardy Diagnostics) were brought to room temperature and 10mm wells were punched

out of the agar (Figure 3.2). The plates were then inoculated with a pre-cultured solution

of 0.5 Mcfarland adjustment (~150e^6 CFU/ml) concentration of *E. coli* using a

densitometer (DensiCheck). Wells were filled with 0.2 grams of copper CMAT, with

CMAT lacking copper, and incubated overnight. Positive and negative controls were

prepared with each experiment. Results were compared to a positive control of the

standard antibiotic ciprofloxacin (concentration 20ug/ml). Plates were incubated

overnight at 37C and 5% carbon dioxide. Next, plates were removed and observed the

following day. Antimicrobial activity assessment was made by measuring the diameter of

the zone of inhibition which formed around each well.
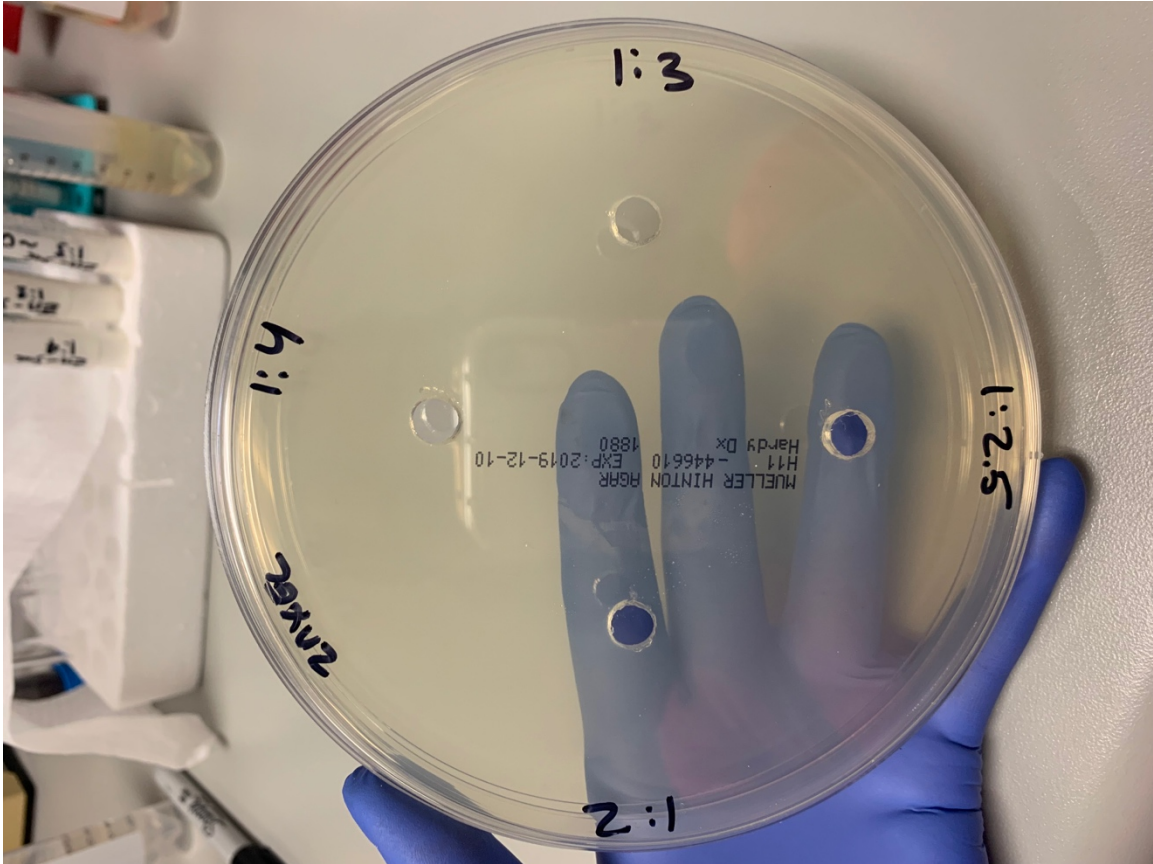
Figure 3.2 Modified Meuller Hinton agar plates containing wells for CMAT susceptibility testing.

Antimicrobial agents, such as chemical antibiotics, exhibit variable concentration-dependent as well as time-dependent effects which can play a role in their effectiveness against a specific organism or group of organisms. Such effects include the minimal inhibitory concentration (MIC), concentration-dependent killing rate, and the post antibiotic effect. The minimum inhibitory concentration is the lowest concentration of an agent that prevents the growth of bacteria [26]. This value dictates whether a specific

bacterial strain is classified as susceptible or resistant to the agent. Some agents, such as

the antibiotic classes fluoroquinolones and aminoglycosides, exhibit an increase in

bacterial killing rate with an increase of agent concentration [26] [27]. A standard

concentration titration was performed and graphed in Figure 3.3 showing how antibiotic

efficacy is exponential against *E. coli* with increasing concentration.
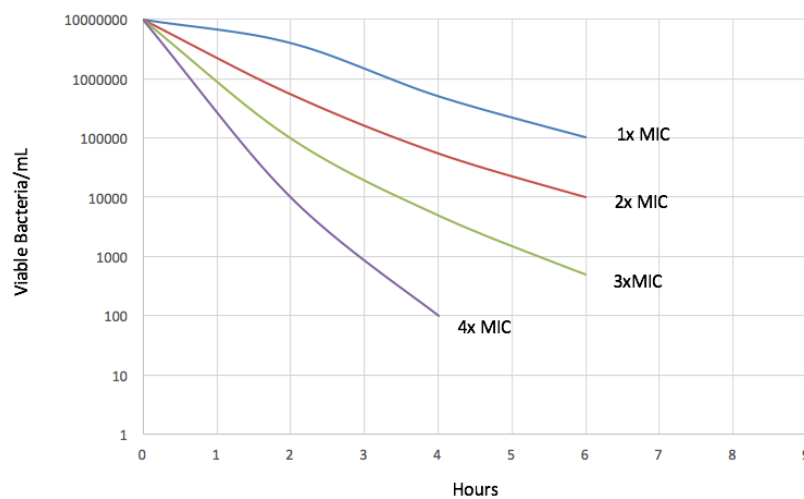
Figure 3.3: Concentration dependent effects of antimicrobial agents. When a 10^6 starting

concentration of *E. coli* is incubated in ciprofloxacin, a concentration dependent killing

rate is observed. An antibiotic concentration doubling results in a ten-fold decrease of

cells.

3.3 Results

Figure 3.5 demonstrates clear diameter zone of inhibition formed around

ciprofloxacin antibiotic disks of 30 millimeters after an eighteen-hour incubation, which

is considered susceptible by standard antibiotic susceptibility testing guidelines [26].

Control plates with no antibiotic showed clear expected growth covering the agar plate.

A clear zone of inhibition is observed surrounding the wells containing CMAT, indicating that *E. coli* exhibits some susceptibility to CMAT (Figure 3.4).
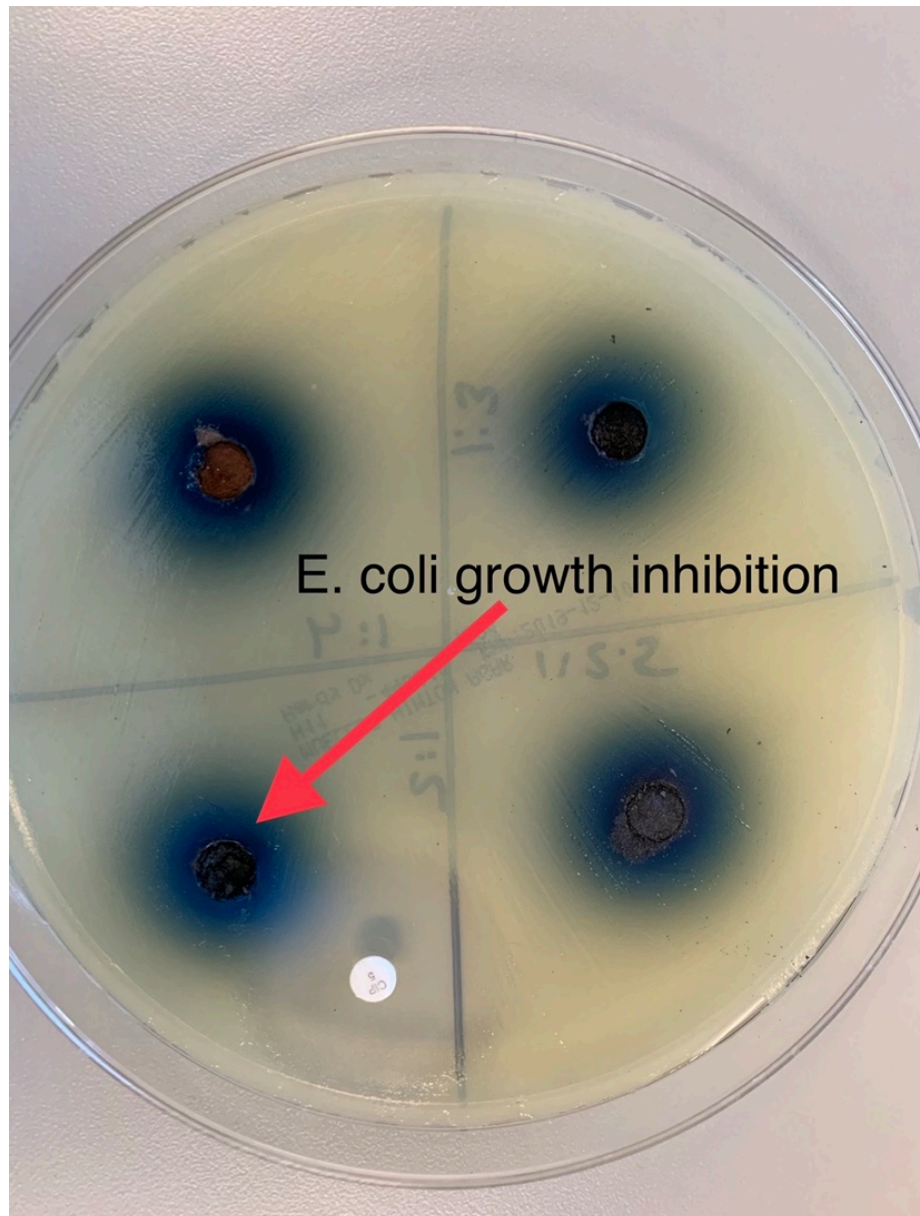
Figure 3.4: Zones of inhibition surrounding CMAT test material where E. coli growth is suppressed following overnight incubation.
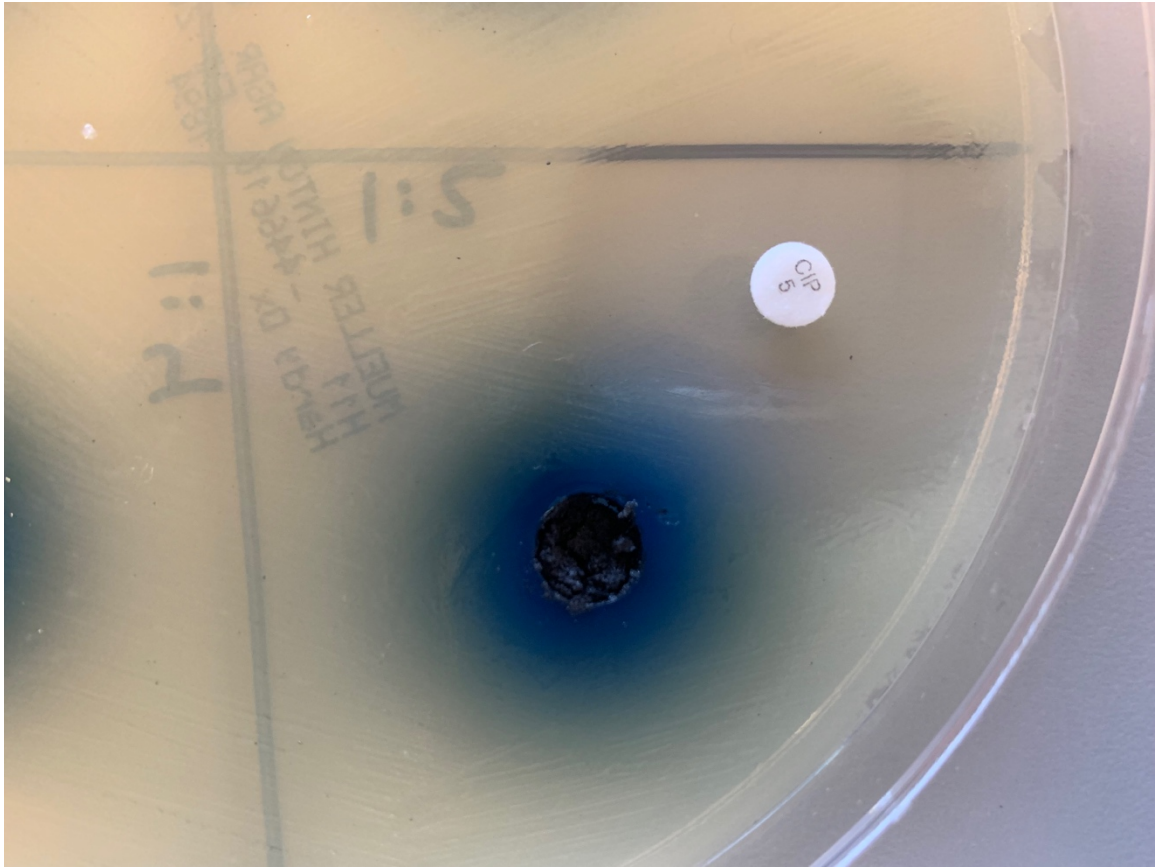
Figure 3.5: Close-up of clearing surrounding CMAT well and ciprofloxacin control. The inhibition zone diameter of 30mm surrounding ciprofloxacin is the current accepted value of susceptibility for *E. coli,* although high rates of resistance is observed in many strains to this conventional antibiotic.
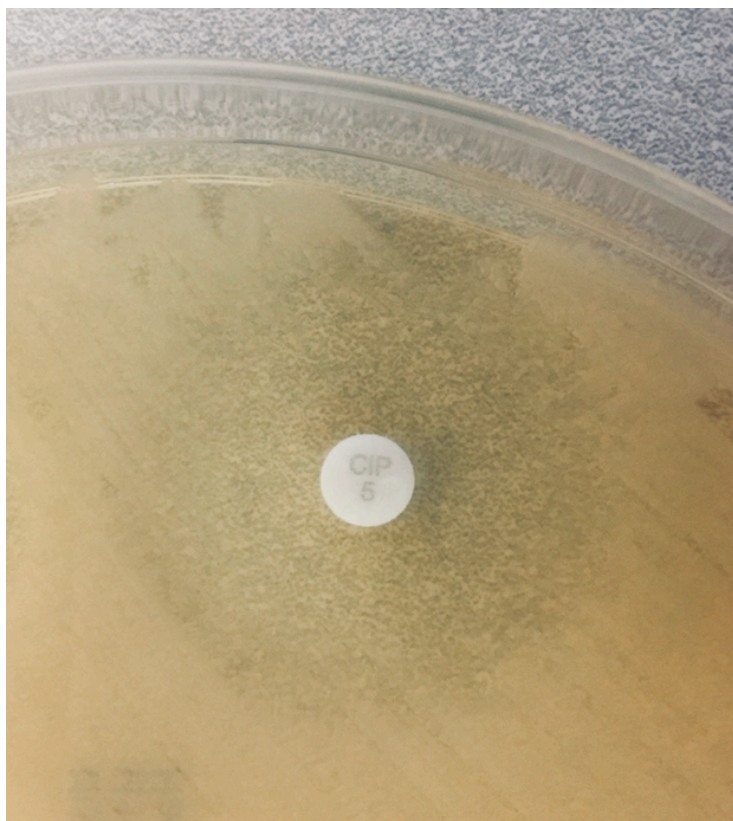
Figure 3.6: Zone of inhibition containing satellite colonies surrounding ciprofloxacin disk in *E. coli* culture on Meuller-Hinton agar demonstrates the active evolution of antibiotic resistance.

3.4 Conclusion

Copper CMAT prevented proliferation of *E. coli* as indicated by growth inhibition zones around the perimeter of copper CMAT deposited on agar plates. This result confirms that copper nanoparticles are actively available in CMAT; the metal particles are not hindered by carbon matrix and may be further processed or functionalized for sensing and therapeutics in addition to antimicrobial applications. Furthermore, CMAT did not demonstrate the rapid evolution of resistance by *E. coli* over time such as the

conventional antibiotic ciprofloxacin. Figure 3.6 shows the shift of E. coli from antibiotic susceptible into antibiotic resistant indicated by the formation of satellite colonies surrounding the antibiotic. *E. coli* did not develop this resistance during the same time period.

Due to the present need for dynamic, inexpensive, and versatile antimicrobial materials, the antimicrobial effects on other common pathogens are investigated. Furthermore, it is helpful to deduce whether the material is bacteriostatic, that it, it prevents bacterial growth as opposed to bactericidal. A more sensitive and reliable technique for quantifying bacterial cells is therefore necessary to compare and measure the activity of the antimicrobial agent in question. A Resazurin-Resofurin viability assay can better measure sensitive changes and cell proliferation.

Chapter 4: Viability and Cell Proliferation Assays

4.1 Introduction

Resazurin is a water soluble, stable, cell membrane permeable dye. It is a non-flurescent dye that is reduced to highly fluorescent resofurin. The dye acts as an electron acceptor and can be reduced by several metabolic compounds including: NADH, FADH, FMNH, and NADPH in addition to cytochromes. The change from the oxidized to reduced state is detected fluorescently or colorimetrically for the detection of viable cells. Resazurin Viability Assays are vastly advantageous because they perform with superior sensitivity and contain a wide dynamic range. Measuring light emitted during a chemical reaction is practical because the light output is a relative quantification of the number of

viable cells. Since cell growth creates a reduced environment and inhibition of growth maintains an oxidized environment, the resazurin assay can be used to reproducible detect cells. Here, bacterial strains Escherichia coli (*E. coli*), Pseudomonas aeruginosa (*P. aeruginosa*), and Staphylococcus aureus (*S. aureus*) are incubated in the presence of copper CMAT and their viabilities are measured by fluorescence of resazurin reactions.

4.2 Methods

E. coli, P. aeruginosa, and *S. aureus* control slants are inoculated in liquid Meuller Hinton broth (Sigma) and incubated overnight at 37 degrees Celsius. Approximately 150 million CFU of each bacterial strain is prepared using optical density measurements and dispensed in a 96-deep well plate containing copper CMAT to a final volume of 1 mL using fresh Meuller Hinton nutrient broth. The deep well plate is incubated on a shaker overnight at 37 degrees Celsius. Following incubation, 100uL of resazurin (Biotium Resazurin Cell Viability Kit) is added to each well of test samples and controls and incubated again for 1 hour at 37 degrees Celsius as outlined in assay kit protocol. Fluorescence is measured using an Eppendorf plate reader with an excitation wavelength of 57nm and emission wavelength of 585nm. Normalization is performed by subtracting background fluorescence measured by the assay blank. Standard curves of titrated control cells are added and measured each experiment. The over incubation of resazurin dye must be carefully avoided to prevent over reduction of resorufin to the non-fluorescent product, hydroresorufin (indicated by color change of pink to colorless).

4.3 Results

No active growth of *E. coli*, *P. aeruginosa*, or *S. aureus* was detected in samples treated with copper CMAT as indicated by normalized RFU measurements (Figure 4.1) following end-point measurements after overnight incubation.
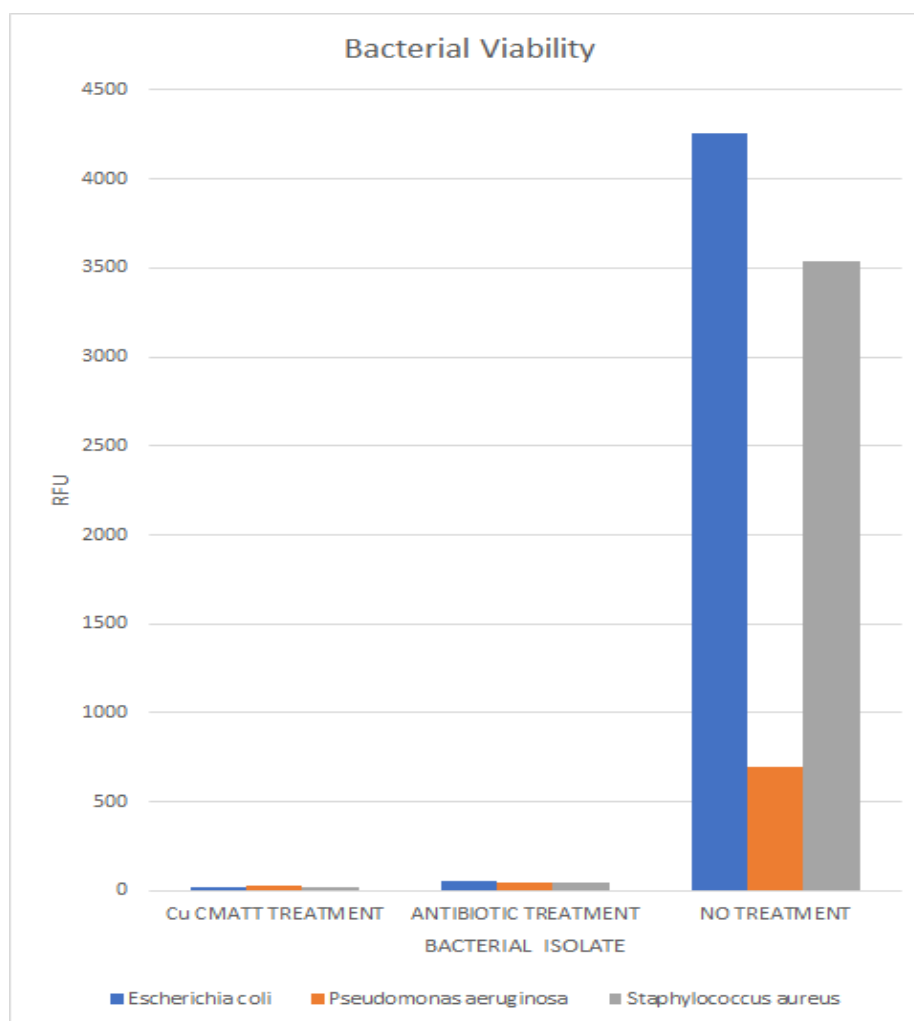
Figure 4.1 Bacterial viability as correlated to relative fluorescence of *E. coli*, *P. aeruginosa*, and *S. aureus* resazurin assays treated with copper CMAT compared to untreated wells.

4.4 Conclusion

Resazurin viability assay results indicate that copper CMAT prevents the growth of *E. coli*, *P. aeruginosa*, and *S. aureus* in vitro. While agar disk diffusion is inherently very subjective due to the dependency of the observer's naked eye to interpret disk zones, resazurin assays are much more sensitive and accurate. Therefore, the antimicrobial [28]properties of CMAT further confirmed by the results of the resazurin viability test. Additionally, these specific test organisms contribute to the cause of most hospital acquired infections worldwide and possess high rates of antibiotic resistance [29]. Therefore, CMAT provides a possible inexpensive, easily manufactured, novel solution as an antibacterial coating material for hospital equipment, floors, and walls effective against these microorganisms.

However, the resazurin viability assay only indicates viable and metabolically active cells and does not consider inactive or dormant cells, which may turn active given the right conditions. It is important to investigate the bacteriostatic and bactericidal capacity of CMAT, and compare the kinetics of CMAT to those of conventional antibiotics by measuring the change in cell growth over time.

Chapter 5. Liquid Broth Culture

5.1 Introduction

The previous antimicrobial experiments have indicated that CMAT can prevent the growth of common bacteria like *E. coli*, *P. aeruginosa*, and *S. aureus*. An important parameter that must be analyzed is the kinetics and type of growth inhibition. Measuring the growth over time can be accomplished by incubating the test sample in liquid broth

27

and dispensing and streaking a fixed volume of the broth onto agar plates at multiple time points. After incubating the agar streak plates overnight, colonies are counted and converted to colony forming units (CFUs) as a measure of bacterial concentration. Any inactivated or stressed cells will also grow and be accounted for in this method since cells are reintroduced into a nutrient rich environment, while truly dead cells are not quantified. This method can reveal if the antimicrobial in question is bacteriostatic or bactericidal. Here, we test copper CMAT against gram positive bacteria, gram negative bacteria, as well as fungus and measure growth rate during incubation in solution containing CMAT.

5.2 Methods

E. coli, P. aeruginosa, and S. aureus, C. parapsilosis, E. faecalis, and K. pneumoniae controls are inoculated in liquid Meuller Hinton broth (Sigma) and incubated overnight at 37 degrees Celsius. Approximately 150 million CFU of each bacterial and fungal strain is measured out using optical density turbidity measurements and dispensed in a 96-deep well plate containing copper CMAT to a final volume of 1 mL using fresh Meuller Hinton nutrient broth. Positive controls of each microorganism are tested in wells without the addition of CMAT and negative controls are prepared with each organism in the presence of its susceptible antibiotic. The plate is incubated on a low speed shaker. Every hour, the plate is removed and 10uL of each sample is dispensed onto agar plates and streaked evenly across the plate with a disposable plastic loop. Time point agar plates and the deep well sample plate are returned to the incubator. A final

aliquot is taken at 12 hours and agar plates are further incubated 18 hours. Colony

forming units are quantified and plotted over time.

5.3 Results

No viable cells were observed by one hour following incubation with copper

CMAT. All positive controls had acceptable growth as seen plotted in Figure 5.3. Figure

5.1b gives a snapshot of *E. coli* after 1 hour incubation with copper CMAT exhibiting a

100% killing rate to 5.1a, *E. coli* positive control (no CMAT treatment).

Additionally, CMAT demonstrated 100% effective killing of the fungal organism,

C. parapsilosis, as seen in the agar plate pictured in Figure 5.2. In Figure 5.2, the fungal

plate is split in half, with growth of the *C. parapsilosis* positive control on the bottom half

and the CMAT treated sample on the top half.
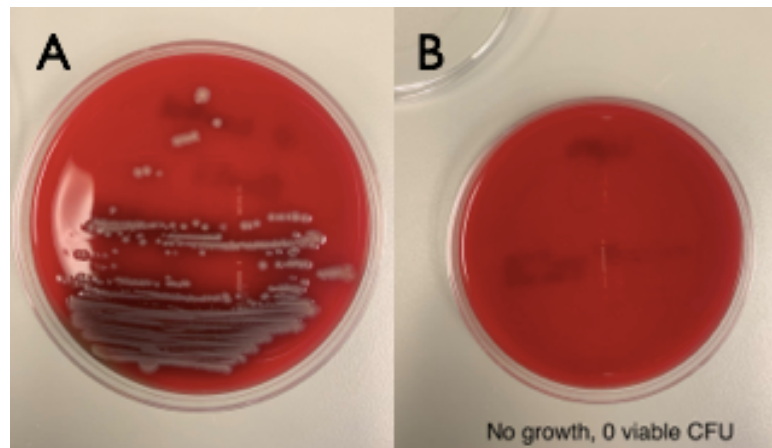
Figure 5.1: Dense growth of *E. coli* positive control (A) compared to *E. coli* after 1 hour

incubation in copper CMAT (B).
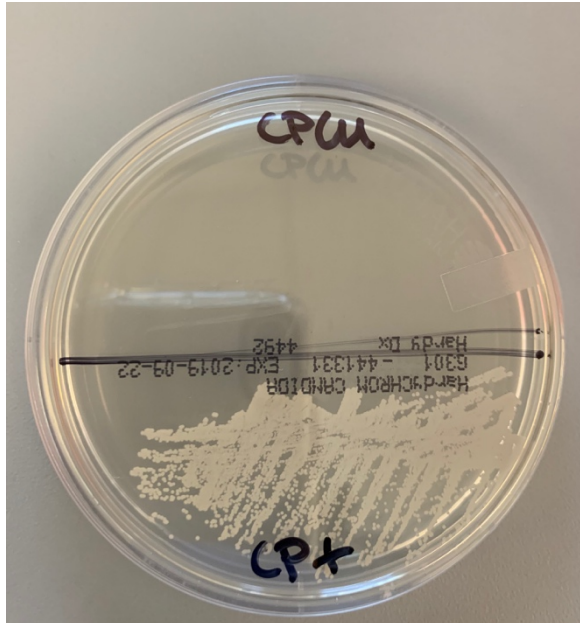
Figure 5.2: Snapshot showing growth of the fungus C. parapsilosis positive control on bottom half of agar plate and C. parapsilosis treated with copper CMAT on top half of the agar plate.

CMAT effectively inhibits the growth of *E. coli, P. aeruginosa, and S. aureus, E. faecalis* earlier and more effectively than their respective antibiotics (Figure 5.4*). K. pneumoniae* shows equal susceptibility to both CMAT (Figure 5.5) and conventional antibiotics (Figure 5.4). In addition to increased susceptibility, no resistance progression is observed to CMAT treatment, whereas the development of antibiotic resistance is common in these microorganisms; *P. aeruginosa* and *E. faecalis* exhibit resistance to the antibiotic Ciprofloxacin by hour 12 in as indicated by increased growth concentration of these organisms by hour 12 in Figure 5.4.
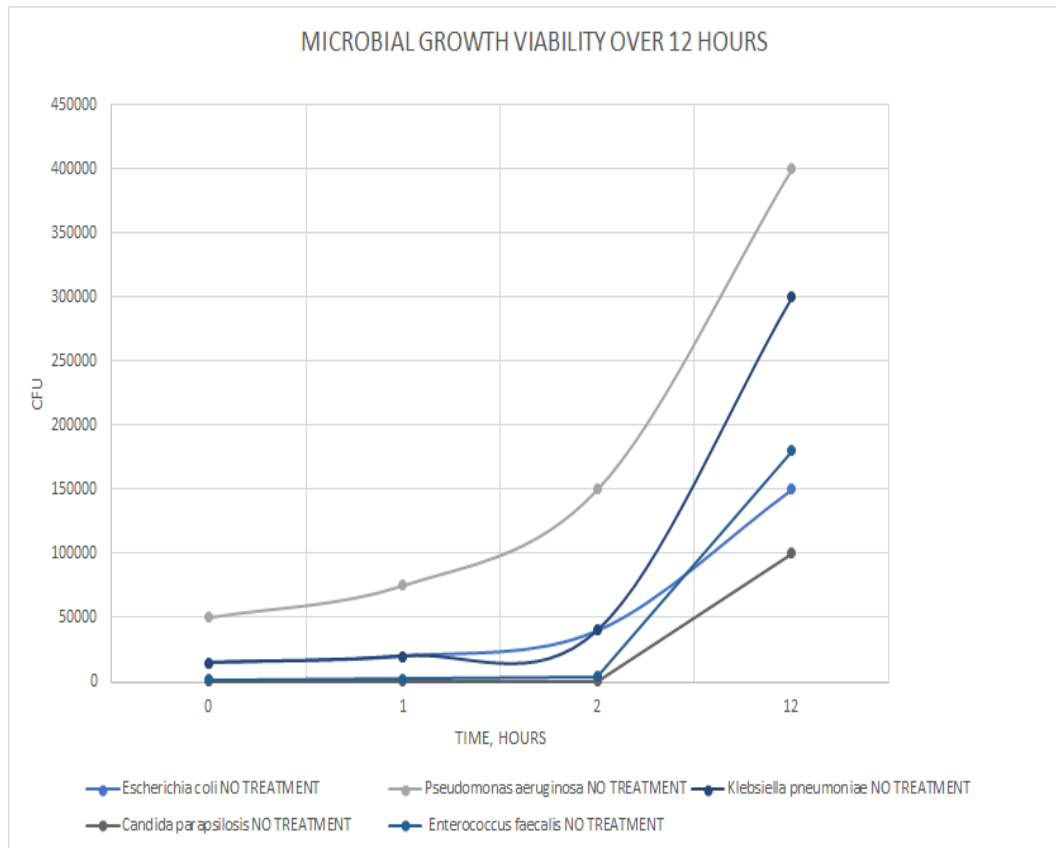
Figure 5.3: Growth of positive controls (no treatment with antimicrobials) plotted over 12 hours of gram negative *E. coli, K. pneumoniae, P. aeruginosa*, gram positive *E. Faecalis,* and the fungus *C. parapislosis*.

Figure 5.4: Viability of microorganisms treated with antibiotics plotted over time.
Enterococcus spp and *Pseudomonas spp* develop resistance by hour 12 indicated by
positive slope over time. These organisms are becoming more and more difficult to treat
due to their well adapted and abrupt antibiotic resistance evolvement characteristics.
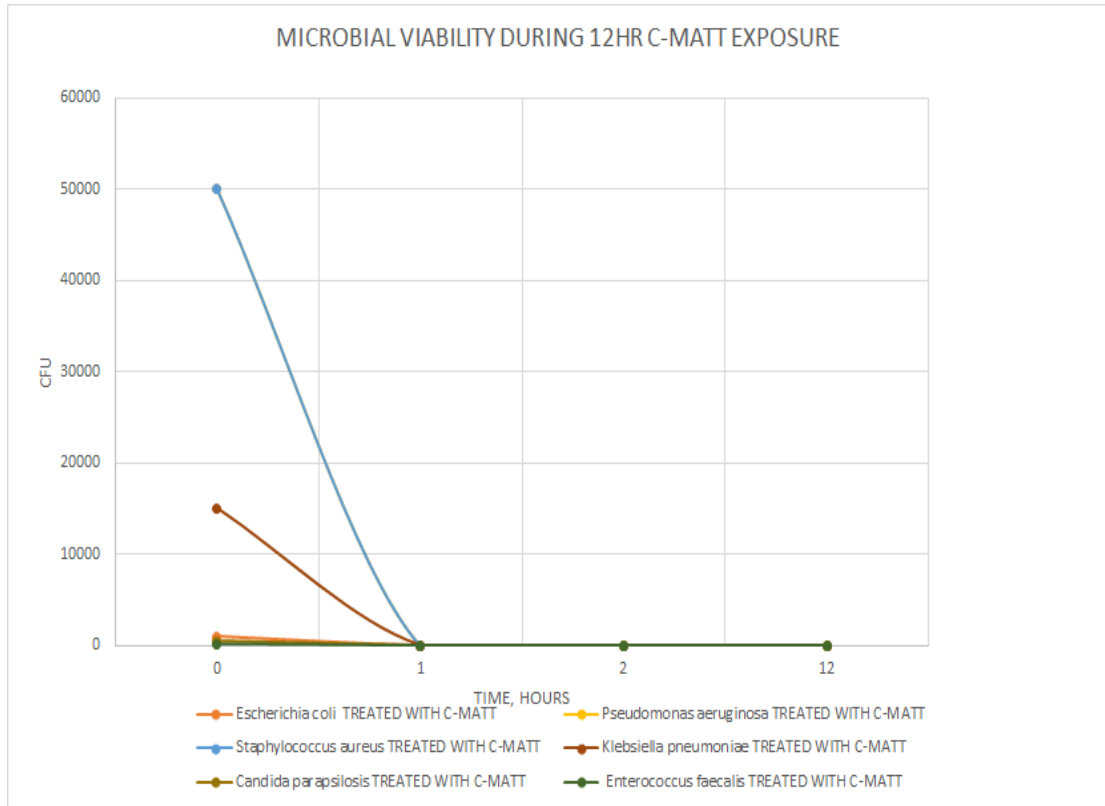
Figure 5.5: Viability of microorganisms treated with copper CMAT plotted over time.

No increase nor re -growth rate is observed in samples treated with CMAT.
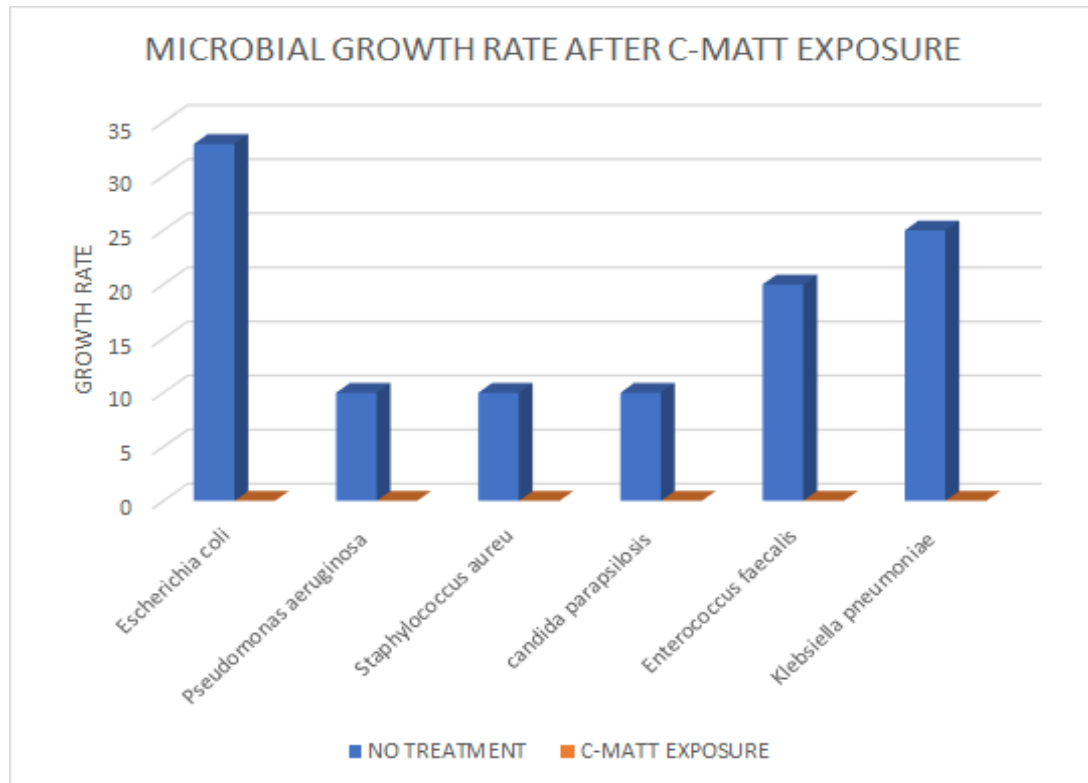
Figure 5.6: Growth rates of microorganisms treated with CMAT compared to no treatment.

5.4 Conclusion

CMAT exhibits effective and quick killing mechanisms on a number of gram positive bacteria, gram negative bacteria, as well as fungi. The bactericidal effects of CMAT here resulted in more effective killing than those of the tested antibiotics; all microbial growth is inhibited by the first hour incubation in CMAT (Figure 5.5). Furthermore, no development of resistance to CMAT is observed, while resistance to conventional antibiotics is actively demonstrated. To broaden the applications of CMAT as an antimicrobial surface coating, it is necessary to test whether this antimicrobial

activity is preserved outside of an aqueous environment and effective as a surface coating antimicroabial.

Chapter 6. Modified Cytotoxicity Fluorescence Assay

6.1 Introduction

Millions of cases of hospital acquired infections occur every year involving difficult to treat bacterial and fungal agents. These pathogens most commonly infect patients through IV lines, intubation, catheters, devices, and medical implants [29]. In effort to improve patient outcomes and provide better infection control, antimicrobial coatings are ideal to apply in clinical settings in addition to aseptic practices. Most efforts involving effective antimicrobial surface technologies are limited by toxicity of exposure due to the diffusion of the toxic agents [28]. Other contributions in literature include profound investigations and design of cationic polymers containing intrinsic antimicrobial activity; the most prominent are those derived from (meth)acrylates containing quaternary ammonium salts [5]. These biocidal polymers are hypothesized to function by establishing electrostatic interactions with the negatively charged cell walls of bacteria leading to cell lysis. However, the antimicrobial activity of these cationic polymers significantly deceases when used as a surface coating due to steric hindrance and immobility, preventing interaction with the microbe [5]. There polymers require a combined system with another antimicrobial agent in a synergistic effort in order to be effective. Therefore, there is a need for effective, manageable, and stable surface immobilized antimicrobial agents as a solution to infection control.

To investigate the antimicrobial effect and activity on a surface treated with CMAT, a modified Live/Dead cytotoxicity assay was designed. Modification of this fluorescence staining technique helps to distinguish surface antimicrobial agents from solution diffusion agents. Figure 6.1 provides a snapshot of E. coli stained with propidium iodide (Live/Dead stain) in solution; live cells stain green whereas dead cells stain red [30]. Here, an inoculation chamber is created with the test substrate and a glass coverslip. CMAT is embedded in PMMA to simulate a surface coating (Figure 6.2) and inoculated with fluorescently stained bacterial cells then coverslipped. Two distinct populations are probed by fluorescence microscopy for viability: cells in solution, and cells adhered to the surface of the test substrate. Effective killing of cells is found only on the substrate surface of truly surface immobilized agents, whereas exclusively diffuse agents result in killing of cells only in solution.
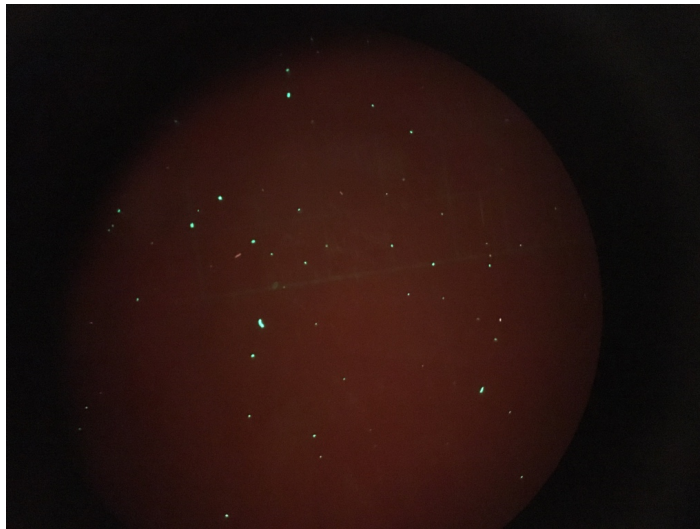
Figure 6.1: Snapshot of *E. coli* dilution sample in solution fluorescently stained with propidium iodide (Live/Dead stain) under a hemocytometer viewed with a 200x

36

Fluorescent in-situ hybridization combo red/green filter microscope for cell quantification and viability.
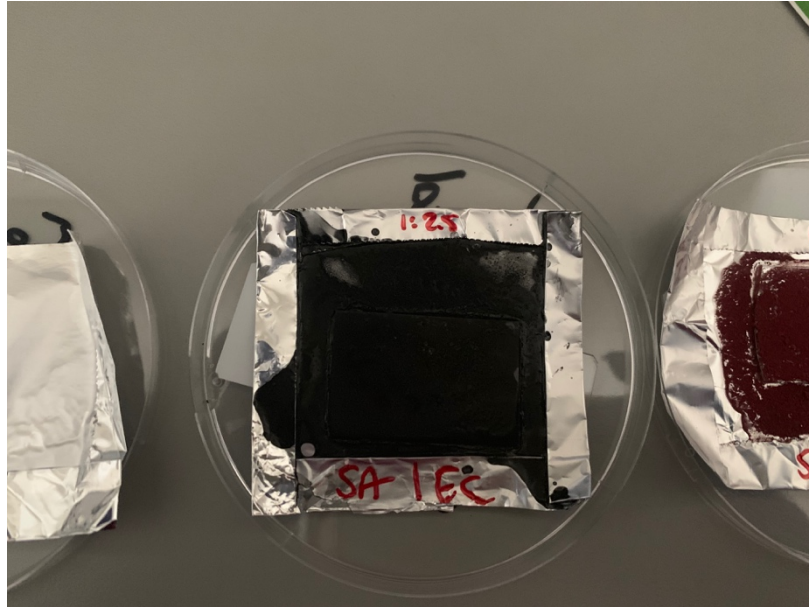
Figure 6.2: CMAT embedded in PMMA surface coating

6.2 Methods

Centrifuge tubes of Meuller Hinton broth were inoculated with slants of E. coli and S. aureus and incubated overnight. The cultures were pelleted in a centrifuge and washed three times in saline. The concentration was adjusted to about 10^7 cfu/ml using optical density.

The Live/Dead stain solutions were prepared from the Baclight Bacterial Viability Kit from Invitrogen. The stain stock solution was prepared by mixing 1.5 μL of propidium iodide stock and equal volume of Invitrogen SYTO9 stock in 97μL saline. 100 μL of the stock solution was then added to 900μL of each washed solution of E. coli and S. aureus and incubated for 15 min. 100 μL of the stained cells were dispensed onto the

surface of CMAT-PMMA and coverslipped. A fluorescent microscope is used to image the samples.

6.3 Results and Conclusion

Immediately following inoculation of PMMA-embedded CMAT with E. coli and S. aureus, the inoculation chambers are visualized with a fluorescence microscope. No live cells are visualized at the surface of CMAT as characterized by red stained cells in Figure 6.3. In addition to PMMA- embedded CMAT coating providing effective killing of *E. coli* and *S. aureus*, killing was observed immediately after contact with the surface. This quick killing action could be a result of direct membrane interaction and cell lysis, opening broad application opportunities as an immobilized, effective antimicrobial surface coating. Some killing was observed in solution portion of chamber, indicating that some agent diffusion is still taking place in PMMA-embedded CMAT coating.
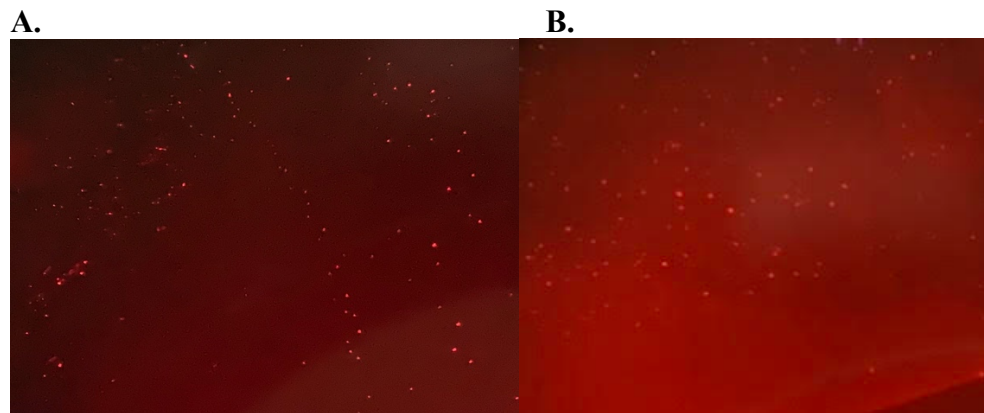
Figure 6.3: (A) *E. coli* stained with Live/Dead kit imaged at surface of PMMA-embedded CMAT. **(B)** *S. aureus* stained with Live/Dead kit imaged at surface of PMMA-embedded CMAT. Dead cells stain red while live cells stain green.

Chapter 7: Conclusion

Here we have described the novel, facile synthesis and characterization of an inexpensive, scalable, copper doped carbon matrix material intended for antimicrobial surface, filtration, and packaging applications. Copper CMAT is a low density and porous carbon foam material of graphitic, amorphous carbons sheathed in ~ 500nm diameter copper and copper oxide nanoparticles. CMAT can be synthesized efficiently with economical resources using straightforward methods. It is easily scalable for high throughput production and manufacturing. Copper CMAT demonstrates excellent antimicrobial properties by inhibiting growth and killing gram positive and gram negative bacteria as well as yeast organisms with no observed development of resistance to CMAT by the tested organisms. Copper CMAT also exhibits bactericidal mechanisms at the material surface level as well as in solution.

In a solution form, CMAT acts as an effective antimicrobial agent via surface killing as well as mobile diffusion. Additionally, PMMA-embedded CMAT as an immobile surface coating retains its antimicrobial effects at the surface level of the material, making CMAT a promising material of antimicrobial applications. Some diffusion may still take place in the presence of liquids, therefore optimization of CMAT as a polymer based coating may be required to eliminate the diffusion of the agent that can be utilized as a non-toxic surface treatment for in-vivo coatings in addition to external coating applications.

References

[1] D. DHaneswar, C. N. Bikash, P. Phukon and K. D. Swapan, "Synthesis and evaluation of antioxidant and antibacterial behaviorof CuO nanoparticle," *Colloids and Surfaces B: Biointerfaces,* vol. 101, pp. 430-433, 2013.

[2] Y. Yuan, Q. Peng and S. Gurunathan, "Effects of silver nanoparticles on multiple drug-resistant strains of Staphylococcus aureus and Pseudomonas aeruginosa from mastitis-infected goats: An alternative approach for antimicrobial therapy," *International Journal of Molecular Sciences,* vol. 18, p. 569, 2017.

[3] World Health Organization, "Antimicrobial Resistance," April 2014. [Online]. Available: www.who.int/drugresistance/ documents/surveillancereport/en. [Accessed 3 March 2018].

[4] G. Yi, Y. Yuan, X. Li and Y. Zhang, "ZnO Nanopillar Coated Surfaces with Substrate-Dependent Superbactericidal Property," *Small,* pp. 1-8, 2018.

[5] A. M.-B. M. A. D. J.-T. H. M.-T. C. G.-S. U. S. S. R. G.-S. Roberto Yañez-Macías, "Combinations of Antimicrobial Polymers with Nanomaterials and Bioactives to Improve Biocidal Therapies," *Polymers,* vol. 11, no. 11, p. 1789, 2019.

[6] AG Scientific, "AG Scientific," 2016. [Online]. Available: http://agscientific.com/blog/2016/03/crispr-cas9/. [Accessed 3 March 2018].

[7] S. Bykkam, S. Narsingam, M. Ahmadipour, T. Dayakar, R. K. Venkateswara, C. Shilpa and S. Kalakotla, "Few layered graphene Sheet decorated by ZnO Nanoparticles for anti-bacterial application," *Superlattices and Microstructures,* vol. 83, pp. 776-784, 2015.

[8] K. Dedkova, B. Janikova, K. Matejova, K. Cabanova, R. Vana, A. Kalup, M. Hundakova and J. Kukutschova, "ZnO/graphite composites and its antibacterial activity at different conditions," *Journal of Photochemistry and Photobiology B: Biology,* vol. 151, pp. 256-263, 2015.

[9] P. Calcagnile, I. Fragouli, S. Bayer, G. C. Anyfantis, P. D. Martiradonna, R. Cozzoli and Athanassiou, "Magnetically driven floating foams for the removal of oil contaminants from water," *ACS Nano,* vol. 6, no. 6, pp. 5413-5419, June 2012.

[10] T. Kievit, M. Parkins, R. Gillis, R. Srikumar, H. Ceri, K. Poole, B. Iglewski and D. Storey, "Multidrug Efflux Pumps: Expression Patterns and Contribution to Antibiotic Resistance in Pseudomonas aeruginosa Biofilms," *Antimicrobial Agents and Chemotherapy,* vol. 45, no. 6, pp. 1761-1770, June 2001.

[11] N. Cioffi, L. Torsi, N. Ditaranto, G. Tantillo, L. Ghibelli, L. Sabbatini, T. Bleve-Zacheo, M. D'Alessio, P. G. Zambonin and E. Traversa, "Copper Nanoparticle/Polymer Composites with Antifungal and Bacteriostatic Properties," *Chem. Mater,* vol. 17, no. 21, pp. 5255-5262, 2005.

[12] J. Hoekstra, A. Beale, F. Soulimani, M. Versluijs, D. van de Kleut, J. Koelewijn, J. Geus and L. Jenneskens, "the effect of iron catalyzed graphitization on the textural properties of carbonized cellulose: Magnestically seperable graphitic carbon bodies for catalysis and remediation," *Carbon,* vol. 107, pp. 248-260, 2016.

[13] F. Moliter, C. Guttinger, S. Stampfer, A. Droscher, T. Jacobsen, T. Ihn and K. Ensslin, "Electronic properties of graphene nanostructures," *J. Phys. Condens. matter an Inst. Phys. J.,* vol. 23, no. 24, p. 243201, 2011.

[14] K. S. Novoselov, V. I. Falko, P. R. Colombo, P. R. Gellert and M. G. Schwab, "A roadmap for graphene," *Nature,* vol. 490, no. 7419, pp. 192-200, 2012.

[15] V. V. e. a. Mody, "Introduction to Metallic Nanoparticles," *Journal of Pharmacy and Bioallied Sciences 2.4,* pp. 282-289, 2010.

[16] G. Ren, D. Hu, E. Cheng, M. Vargas-Reus, P. Reip and R. Allaker, "Characterisation of copper oxide nanoparticles for antimicrobial applications.," *International Journal of Antimicrobial Agents,* vol. 33, no. 6, pp. 587-590, June 2009.

[17] R. Sivaraj, P. Rahman, P. Rajiv, S. Narendhran and R. Venckatesh, "Biosynthesis and characterization of Acalypha indica mediated copper oxide nanoparicles and evaluation of its antimicrobial and anticancer activity," *Spectrochimica Acta Part A: Molecular and Biomolecular Spectroscopy,* vol. 129, pp. 255-258, 2014.

[18] R. N. Chopra, S. L. Nayar and I. C. Chopra, Glossary of Indian medicinal plants, New Delhi: Council of Scientific and Industrial Research, 1956.

[19] D. P. Z. M. P. R. M. O. C. S. O. Hamed Hosseini Bay, "Scalable multifunctional ultra-thin graphite sponge: free-standing, superporous, superhydrophobic, oleophilic architecture with ferromagnetic properties for environmental cleaning," *Nature,* vol. 6, p. 21858, 2016.

[20] D. Brownson, D. K. Kampouris and C. E. Banks, "An overview of graphene in energy production and storage applications," *J. Power Sources,* vol. 196, no. 11, pp. 4873-4885, 2011.

[21] A. C. Ferrari and J. Robertson, "Raman spectroscopy of amorphous, nanostructured, diamond-like carbon, and nanodiamond," *Phil. Trans. R. Soc. Lond. A,* vol. 362, pp. 2477-2512, 2004.

[22] Y. Sato, M. Kamo and N. Setaka, "Raman Spectra of carobons at 2600-33001/cm region," *Carbon,* vol. 16, no. 4, pp. 279-280, 1978.

[23] M. Sani Usman, M. Ezzat el, Zowalaty, S. Kamyar, N. Zainuddin, M. Salama and N. A. Ibrahim, "Synthesis, characterization, and antimicrobial properties of copper nanoparticles," *International Journal of Nanomedicine,* vol. 8, pp. 4467-4479, 2013.

[24] B. Adak, P. Nash and D. Chen, "Microstructural characterization of laser cladding of Cu-30Ni," *Journal of Materials Science,* vol. 40, pp. 2051-2054, 2005.

[25] J. M. Garland and A. Halestrap, "Energy Metabolism during Apoptosis," *Journal of Biological Chemistry,* vol. 272, pp. 4680-4688, 21 February 1997.

[26] K. Zeiler and K. Grohe, The In Vitro and In Vivo Activity of Ciprofloxacin, Current Topics in Infectious Diseases and Clinical Microbiology ed., vol. 1, Springer

Fachmedien Wiesbaden, 1986, pp. 14-18.

[27] G. Cheng, H. Hao, M. Dai, L. Zhenli and Z. Yuan, "Antibacterial action of quinolones: From target to network," *European Journal of Medicinal Chemistry,* vol. 66, pp. 555-562, 2013.

[28] R. R. K. K. M. A. J. R. Hironobu Murata, "Permanent, non-leaching antibacterial surface--2: how high density cationic surfaces kill bacterial cells," *Biomaterials,* vol. 28, no. 32, pp. 4870-4879, 2007.

[29] E. J. R. C. H. T. G. R. P. D. C. D. Klevens R, "Estimating health care-associated nfections and deaths in US hospitals, 2002," *Public Health Rep,* no. 122, pp. 160-166, 2007.

[30] S. B. P. W. C. T. F. M. L. M. A. N. S. S. John-Bruce D Green, "Antimicrobial Testing for Surface-Immobilized Agents With a Surface-Seperated Live-Dead Staining Method," *Biotechnology and Bioengineering,* vol. 108, no. 1, pp. 231-236, 2010.

[31] J. Chida, K. Yamane and H. Kido, "An efficient extraction method for quantitation of adenosine triphosphate in mammalian tissues and cells," *Analytica Chimica Acta,* vol. 727, pp. 8-12, 2012.

[32] S. Ray, D. Anand, S. Purwar, A. Samanta, K. Upadhye, P. Gupta and D. Dhar, "Association of high mortality with extended-spectrum beta-lactamase (ESBL) positive cultures in community acquired infections," *Journal of Critical Care,* vol. 44, pp. 255-260, 2018.

[33] H. S. Hsu, P. E. Lu, C. W. Chang, S. J. Sun, C. H. Lee, Y. Y. Chin, H. J. Lin, C. T. Chen and M. J. Huang, "Tunable interfacial magnetic-optical properties of Co doped amorphous carbon film induced by charge transfer after acid treatment," *Carbon,* vol. 77, pp. 398-404, October 2014.

[34] A. Studer, L. Limbach, L. Van Duc, F. Krumeich, E. Athanassiou , L. Gerber, H. Moch and W. Stark, "Nanoparticle cytotoxicity depends on intracellular solubility: Comparison of stabilized copper metal and degradable copper oxide nanoparticles," *Toxicology Letters,* vol. 197, no. 3, pp. 169-174, 2010.

[35] M. Sibag, S. Kim, C. Kim, H. Kim and J. Cho, "Interference sources in ATP bioluminescence assay of silica nanoparticle toxicity to activated sludge," *Journal of Microbiological Methods,* vol. 113, pp. 65-71, 2015.

[36] S. Finger, C. Weigand, H. Buschmann and U. Hipler, "Antimicrobial properties of cyclodextrin–antiseptics-complexes determined by microplate laser nephelometry and ATP bioluminescence assay," *International Journal of Pharmaceutics,* vol. 436, pp. 851-856, 2012.

[37] L. Zhang, Y. Jiang, Y. Ding, M. Povey and D. York, "Investigation into the antibacterial behaviour of suspensions of ZnO nanoparticles (ZnO nanofluids)," *Journal of Nanoparticle Research,* vol. 9, pp. 479-489, 2007.

[38] I. Ruiz, A. George, W. Wang, C. S. Ozkan and M. Ozkan, "Silicon oxide contamination of graphene sheets synthesized on copper substrates via chemical

vapor deposition.," *Adv. Sci. Eng. Med.,* vol. 6, pp. 1070-1075, 2014.

[39] J. Lin, Y. Wu, R. Bi and H. Guo, "All-solid-state microscale lithium-ion battery fabricated by a simple process with graphene as anode," *Sensors & Actuators: A. Physical,* vol. 253, pp. 218-222, 2017.

[40] A. K. Geim and K. S. Novoselov, "The Rise of Graphene," *Nat. Mater.,* vol. 6, no. 3, p. 183=191, 2007.

[41] H. Mattevi, K. Chhowalla and M. Chhowalla, "A review of chemical vapour deposition of graphene on copper," *J. Mater. Chem,* vol. 21, no. 10, p. 3324, 2011.

[42] X. Yang, P. He and Y. Xia, "Preparation of mesocellular carbon foam and its application for lithium/oxygen battery,," *Electrochem. commun,* vol. 11, no. 6, pp. 1127-1130, 2009.

[43] X. Dong, Y. Chen, M. J. Wang, X. Chan-Park, L. Liu, W. Wang, W. Huang and P. Chen, "Superhydrophobic and superoleophilic hybrid foam of graphene and carbon nanotube for selective removal of oils or organic solvents from the surface of water," *Chem. Commun. (Camb),* vol. 48, no. 86, pp. 10660-10662, 2012.

[44] D. Nguyen, N. Tai, B. Lee and S. Kuo, "Superhydrophobic and superoleophilic properties of graphene-based sponges fabricated using a facile dip coating method," *Energy Enviorn. Sci.,* vol. 5, no. 7, p. 7908, 2012.

[45] Biomedical Key, "Principles of Antimicrobial Chemotherapy," Biomedical Key, 1 January 2017. [Online]. Available: https://basicmedicalkey.com/principles-of-antimicrobial-chemotherapy-2/. [Accessed 3 March 2018].

[46] S. Crouch, R. Kozlowski, K. J. Slater and J. Fletcher, "The use of ATP bioluminescence as a measure of cell proliferation and cytotoxicity.," *J. Immunol Methods,* vol. 160, pp. 81-88, 1993.

[47] E. Beutler and M. C. Baluda, "Simplified determination of blood adenosine triphosphate using the firefly system," *Blood,* vol. 23, pp. 688-698, 1964.

[48] A. Lundin, Clinical and Biochemical Luminescence, New York: Dekker, 1982, p. 43.

[49] H. Van de Werf and W. Verstraete, Analystical Applications in Bioluminescence and Chemiluminescence, London: Academic Press, 1984, p. 33.

[50] B. Lee, "Forbes," 19 February 2017. [Online]. Available: https://www.forbes.com/sites/brucelee/2017/02/19/bill-gates-warns-of-epidemic-that-will-kill-over-30-million-people/#4d3cfe4f282f. [Accessed 3 April 2018].

[51] n. Mansur-Azzam, Z. Hosseinidoust, S. Woo, R. Vyhnalkova, A. Eisenberg and T. Van de Ven, "Bacerial survival probability in bactericidal filter paper," *Colloids Surf B Biointerfaces,* vol. 1, no. 117, pp. 383-388, 1 May 2014.

[52] Y. de Rautlin de la Roy, N. Messedi, G. Grollier and B. Grignon, "Kinetics of Bactericidal Activity of Antibiotics Measured by Luciferin-Luciferase Assay," *Journal of Bioluminescence and Chemiluminescence,* vol. 6, pp. 193-201, 1991.

[53] E. Giraud, A. Cloeckaert, D. Kerboeuf and E. Chaslus-Dancla, "Evidence for Active

Efflux as the Primary Mechanism of Resistance to Ciprofloxacin in Salmonella Enterica Typhimurium," vol. 44, no. 5, pp. 1223-1228, May 2000.

[54] J. Roszak, J. Catalan, H. Jarventaus, H. Lindberg, S. Sunhonen, M. Vippola and N. H. Stepnik, "Effect of particle size and dispersion status on cytotoxicity of zinc oxide in human bronchial epithelial cells," *Mutation Research/Genetic Toxicology and Enviornmental Mutagenesis,* vol. 805, pp. 7-18, 2016.

[55] D. Kozak, R. Sergiienko, E. Shibata, A. Iizuka and T. Nakamura, "Non-electrolytic synthesis of copper oxide/carbon nanocomposite by surface plasma in super-dehydrated ethanol," *Scientific Reports,* vol. 6, pp. 1-9, 2016.

[56] K. S. Novoselov, A. Geim, D. J. Morozov, S. V. Zhang, I. V. Dubonos, I. V. Grigorieva and A. Firsov, "Electriv Field Effect in Atomically Thin Carbon Films," *Science,* vol. 306, pp. 666-669, 2004.

[57] J. R. Kyle, C. S. Ozkan and M. Ozkan, "Industrial graphene metrology," *Nanoscale,* vol. 4, no. 13, pp. 3807-3819, 2012.